Quasi-Static Loads for a Helical Gear

Karthik Narayanan Nair

23rd January 2023

Computer-Aided Conception and Production
in Mechanical Engineering

Matriculation Number - 415569

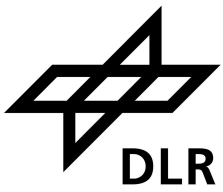

Contents

List of symbols

DEF	Number of times the range of fd_c is split
F	Force
F_a	Axial gear tooth forces
F_r	Radial gear tooth forces
F_t	Tangential gear tooth forces
fd	Face distance
fd_0	Minimum value of face distance
fd_m	Maximum value of face distance
fd_c	Curent value of contact line intercept
fd_a	farthest intercept of contact line in the contact region
f_{load}	Interpolated Function for load
f_{pos}	Interpolated Function for left contact region
g_{pos}	Interpolated Function for right contact region
l	Load in force per unit length
m_{rdx}	Slope of Roll distance
R_b	Base Circle Radius
ra	Roll angle
ra_0	Minimum value of roll angle
ra_m	Maximum value of roll angle
rd	Roll distance
RPM	Rotations per minute
Z_t	Number of teeth
α	Pressure Angle
β	Helix Angle
Δ	Change in fd for each segment of contact line
ψ	Involute roll angle
Θ_{teeth}	Angle between two neighbouring teeth
θ_{lm}	Angle of the left contact teeth to vertical
θ_{rm}	Angle of the right contact teeth to vertical
θ_k	Angle between normals at point k and at the pitch circle

List of acronyms

2D	Two-dimensional
3D	Three-dimensional
AGMA	American Gear Manufacturers Association
CT2D	Clough-Tocher 2D
FEA	Finite Element Analysis
FEM	Finite Element Method
ISO	International Organization for Standardization
LP	Low-Pressure
RMS	Root Mean Square

1 Introduction

Gears are one of the most efficient and widely used methods for transmitting power between two shafts. Gear transmission systems are integral to modern drivetrains in applications such as jet engines. Geared turbofan engines are one of the latest innovations in jet propulsion systems enabled by the development of high-quality gears. Unlike conventional turbofan engines, geared turbofan engines use a planetary reduction gearbox to separate the shafts of the fan and the Low-Pressure (LP) turbine. This mechanism enables an increased efficiency (by allowing higher volume intake of air with a larger diameter) of the fan and reduced weight (by having fewer compressor stages due to increased efficiency). These engines have fewer parts to maintain and are quieter than conventional turbofans [1].The epicyclic gear system connecting the low-speed fan and the compressor-turbine shafts plays a crucial role in operating these engines. Ensuring the reliability of these gears is of utmost importance in this engine.

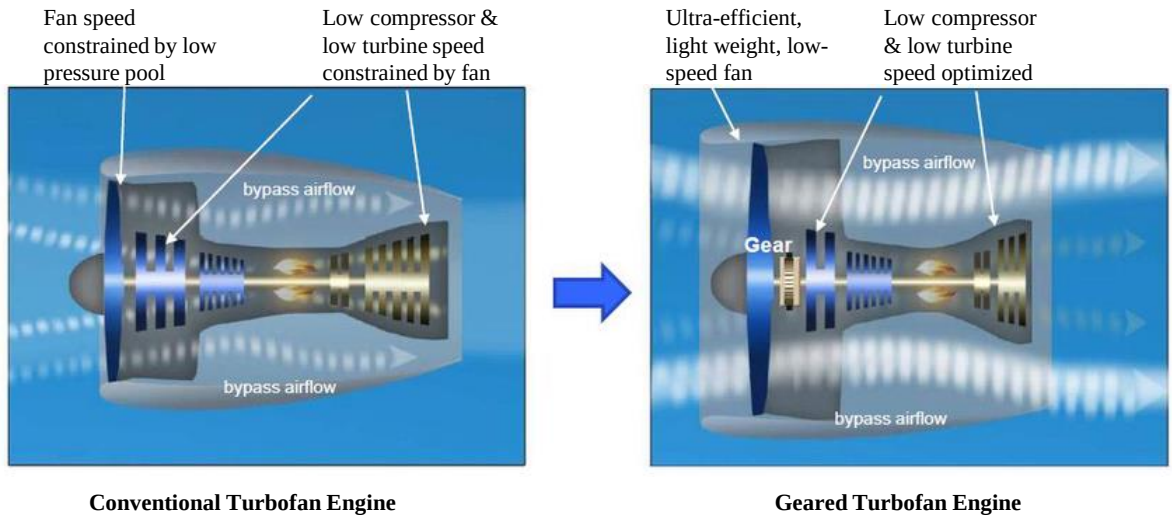

Figure 1: Comparison between conventional and geared turbofan engine architecture [1]

For general use cases, American Gear Manufacturers Association (AGMA) and International Organization for Standardization (ISO) have provided standards for gear design [2, 3, 4, 5, 6]. These standards help ensure consistency and quality in gears for their intended use. But the recommended calculations for gear stresses and failure under these standards are not accurate, especially for complex gear geometries used in many applications. Finite Element Analysis (FEA) helps improve efficiency while detecting failure modes in gear systems. Finite Element Method (FEM) is used to analyse the behaviour of gears for various gear designs, materials and loading conditions, including those encountered in a geared turbojet engine. Its effectiveness and reliability in predicting gear behaviour are well known. For instance, Modi et al. [7] conducted the optimisation and fatigue analysis for a helical gear using FEM for 30 different materials to find the best material for their application.

A quasi-static analysis is a simulation technique used to predict the behaviour of a system under load conditions that change slowly over time. Compared to complete dynamic simulation, they are simple, fast and computationally efficient. A quasi-static FEA analysis provides results that are more accurate than AGMA standard equations. In the context of gear teeth, quasi-static analysis is used to evaluate the stress and deformation of gear teeth under various loading conditions, such as those experienced during gear meshing and transmission. The quasi-static load on a gear tooth face is the average load applied to the tooth over time as the gear rotates and transmits power. This load is determined by considering the various forces that act on the gear teeth, including the normal force between the teeth, the tangential force caused by the power transmission, and any external forces that may be applied. The quasi-static method allows fast simulations of the behaviour of helical gears [8]. A quasi-static model on an ANSYS workbench has been developed by Lias et al. [9] to analyse the time-varying strength of a spur gear system. They investigated the critical location of different strength properties to observe the weakest point of the tooth section. A quasi-static FEM model with three teeth gear has been used over dynamic FEM as it is less sensitive to Normal contact stiffness, penetration tolerance and mesh density. Tooth surface contact stress is measured at the observed teeth in a single mesh cycle for the time interval of engagements. Tooth root bending stress is measured over the flanks area of the observed tooth for single mesh cycles of the gears. The study draws a relationship between the peak stress and the loading position on the tooth. As the quasi-static modelling approach has been validated against the AGMA formulation, the study concluded that the method is reliable for simulating spur gear in time-varying strength analysis. A study to estimate gear load capacity using quasi-static FEM has been conducted by Zhan et al. [8]. Contact type and interface treatment are defined to increase the possibility of solution convergence and to reduce sensitivity to contact stiffness. Boundary conditions facilitate a low step value of rotational velocity. A system damping value of 0.1 is used for quasi-static analysis with inertial effects deactivated. Overall, the literature discussed here clearly shows that quasi-static simulations are an effective tool for the simulations of gears.

1.1 Objectives of the work

The primary goal of this work is to calculate the time-varying loads on the gears over a complete mesh cycle for a quasi-static analysis of a double helical gear. The simulation analyses the test rig of a planetary gear used in the epicyclic gear system of a turbojet engine under the load condition of general running. The load calculation for the static simulations derives from the quasi-static load represented by the uniformly varying loads on the surface of the gear tooth. The load format is shown in Table 2. The values in the cells show peak load at their corresponding roll angle and face distance.

Load per unit length (N/mm)		Face distance (mm)																	
		0	4	8	12	16	20	24	28	32	36	40	44	48	52	56	60	64	68
Roll angle (deg)	23	200	200	200	200	200	200	200	200	200	200	200	200	200	200	200	200	200	200
	24	200	220	220	220	220	220	220	220	220	220	220	220	220	220	220	220	220	200
	25	200	220	240	240	240	240	240	240	240	240	240	240	240	240	240	240	220	200
	26	200	220	240	260	260	260	260	260	260	260	260	260	260	260	260	240	220	200
	27	200	220	240	260	280	280	280	280	280	280	280	280	280	280	260	240	220	200
	28	200	220	240	260	280	280	280	280	280	280	280	280	280	280	260	240	220	200
	29	200	220	240	260	260	260	260	260	260	260	260	260	260	260	260	240	220	200
	30	200	220	240	240	240	240	240	240	240	240	240	240	240	240	240	240	220	200
	31	200	220	220	220	220	220	220	220	220	220	220	220	220	220	220	220	220	200
	32	200	200	200	200	200	200	200	200	200	200	200	200	200	200	200	200	200	200

Table 2: Format of the Load - Normalised

Further, the values of roll angles and face distances that were active in three separate instances are also provided. This data gives information about the travel direction of the line of contact. A representation of this data is shown in Figure 2. Further, the loads are provided in force per unit length (in units N/mm) over the contact region that have to be converted to nodal force values (in units N) for FEA. The test gear would be modelled as a Three-dimensional (3D) solid body, and the loads are applied to the gear's tooth surface. The FEA would solve for the displacement and stress within the gears under these applied loads, allowing evaluation of the peak stress and failure points under these operating conditions.

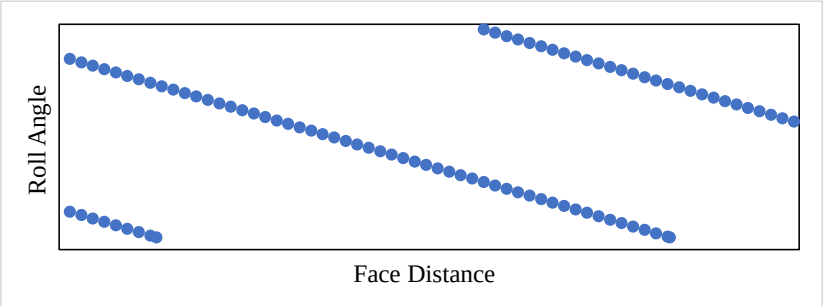

Figure 2: Representation of the data provided for the line of contact on the gear tooth surface

2 Fundamentals of the technology

In this section, the fundamentals of the techniques and technology used in this work are discussed in detail.

2.1 Gear basics

Gears are mechanical components that transmit power and motion between machines and devices. They consist of a set of interlocking teeth around the circumference of a cylindrical or conical shape. When the gears have meshed together, the teeth of the gears engage with each other causing the gears to rotate relative to each other. They have higher efficiency when compared to belts and pulleys while being precise, durable and versatile. Gear design has been known to be very complicated, and with improvements in gear technology, they have become considerably quieter and more powerful. In geared turbojet engines, the individual gears in the epicyclic gear system are double-helical - a gear with a tooth profile that resembles two helical gears meshed together. Double-helical gears have lower noise levels because of engagement happening in small increments, as opposed to spur gears, which engage the entire face simultaneously.

Additionally, these gears can handle much higher loads because of the angled positioning of their teeth. Double helical gears have zero axial thrust forces because the axial forces acting on the right and left-hand twists cancel each other. The performance and reliability of a gear system are affected by various factors, which include the gear geometry, the material properties and the loads. The gear geometry, such as the tooth profile, pitch, and pressure angle, can affect the load capacity, efficiency, and smoothness of operation. The loads, such as the torque and speed, can affect the stress and wear on the gear teeth. The material properties, such as the strength and hardness of the gear teeth, can affect the durability and resistance to wear. The bending and surface strength of the gear tooth are the main contributors to gear failure.

2.2 Geometry of the gear

Helical gears are a type of cylindrical gear with helical teeth that are inclined at an angle to the gear's axis. As discussed in subsection 2.1, this inclination allows for smooth and quiet transmission of torque, making them suitable for power transmission systems. The geometry of a helical gear is defined by parameters such as pitch diameter, tooth angle, pressure angle, pitch and helix angle. The pitch radius R_b is the radius of the pitch circle which is the imaginary circle that rolls without slipping with a pitch circle of a mating gear. The pitch is the distance from one point on a tooth to the corresponding point on the adjacent tooth, measured along the pitch circle. Various tooth forms can be used in helical gears, including modified involute, circular arc, and cycloidal.

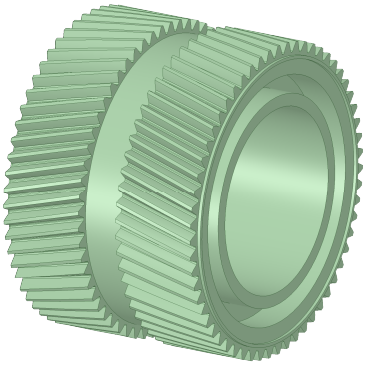

Figure 3: Gear geometry

However, involute gears are the most widely used due to their ease of manufacture. Thus, the gear used in this study is involute. The base circle of an involute gear is the circle from which involute tooth profiles are derived. The line of action of a gear is the path that the point of contact between two meshing gears follows as the gears rotate. The rolling line of an involute gear is the common tangent line of the base circle to the point of contact.

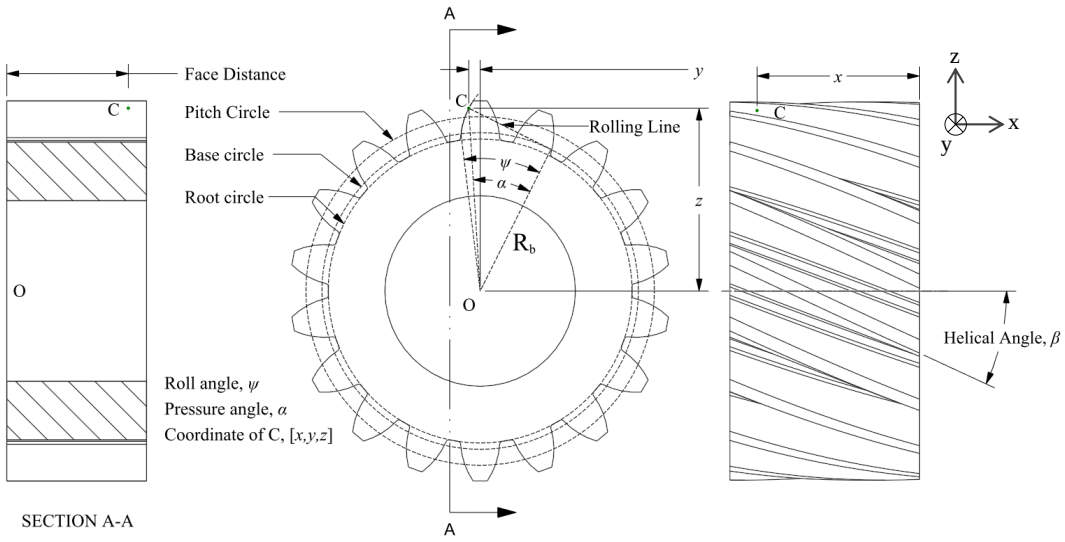

Figure 4: Geometry of an involute gear

In the planned quasi-static analysis, the locating points on the surface of an involute helical gear tooth are critical for applying loads accurately on the contact surface. Roll angle, face distance, and the helix angle at any given point are used to describe the geometric positions of all points on the tooth flank. A random point C, with coordinates (x, y, z), is selected on the surface of the gear tooth in the region of contact. Figure 4 shows a helical gear with a pitch circle, base circle, root circle and rolling line marked. It illustrates the sketch of a spur gear with a cross-section of the spur gear. A helical gear with the same profile and cross-section as the spur gears is shown in the third sketch. Since the gear profile is involute, the normal from point C is a tangent of the base circle. The roll angle of an involute ψ is the angle made by the rolling line on the centre of the

base circle of the gear. The pressure angle for an arbitrary point on an involute curve α is the angle between its radius vector and line tangent to the involute. The helix angle β is the angle between the gear axis and the helix of the teeth.

The relationship between the roll angle and pressure angles

$$\psi = tan(\alpha) - \alpha \tag{1}$$

which is called the involute equation [10].

The parametric equations for the involute curve are

$$z(\psi) = R_b(cos(\psi) + \psi \cdot sin(\psi)) \tag{2}$$

$$y(\psi) = R_b(sin(\psi) - \psi \cdot cos(\psi)) \tag{3}$$

for a base circle of radius R_b.

Simplification of (2) and (3), leads to the equation

$$\psi = \sqrt{\frac{y^2 + z^2}{R_b^2} - 1} \tag{4}$$

The involute angle of a gear can be calculated using the y and z coordinates of any point. The roll angle is independent of the y and z coordinates but directly depends on the distance from the origin. For a spur gear, the face distance fd equals the x coordinate. However, for a helical gear, face distance

$$fd = \frac{x}{cos(\beta)} \tag{5}$$

is related to a helical angle β.

Using (4) and (5), the face distance and roll angle are calculated for any point on the surface of the gear tooth. However, one must ensure that the origin used in the calculation is located on the axis of the gear at a plane where the face distance is zero. If the origin is not there, coordinate transformation must be done. Further, the points taken for calculation must be on the involute surface of the gear tooth. Results achieved for any other location will be inaccurate.

2.3 Interpolation of dense data

Interpolation is a mathematical method used to estimate the value of a point within a continuous domain based on the known values of surrounding points. Interpolation is used in data analysis for estimating missing values in a dataset or to smooth out noise. In this study, inputs for interpolation form a region of dense data. Dense data refers to a dataset in which many observations or measurements are densely packed. There are many different interpolation methods, including linear, polynomial and spline. The choice of interpolation method depends on the specific application and the characteristics of the data. For this study, Clough-Tocher interpolation and Linear n-dimensional Interpolation are used.

2.3.1 Clough-Tocher interpolation

Clough-Tocher interpolation is an interpolation method that is constructed by triangulating the input data points followed by a piecewise cubic polynomial for each triangle. It is a popular method for interpolating gridded data because it produces smooth, continuous solution and is relatively simple to implement. The results of this interpolation are guaranteed to be continuously differentiable which makes it useful for creating data that needs to be further differentiated. To perform Clough-Tocher interpolation, the data points in the domain are first divided into non-overlapping triangles using Delaunay triangulation algorithm.

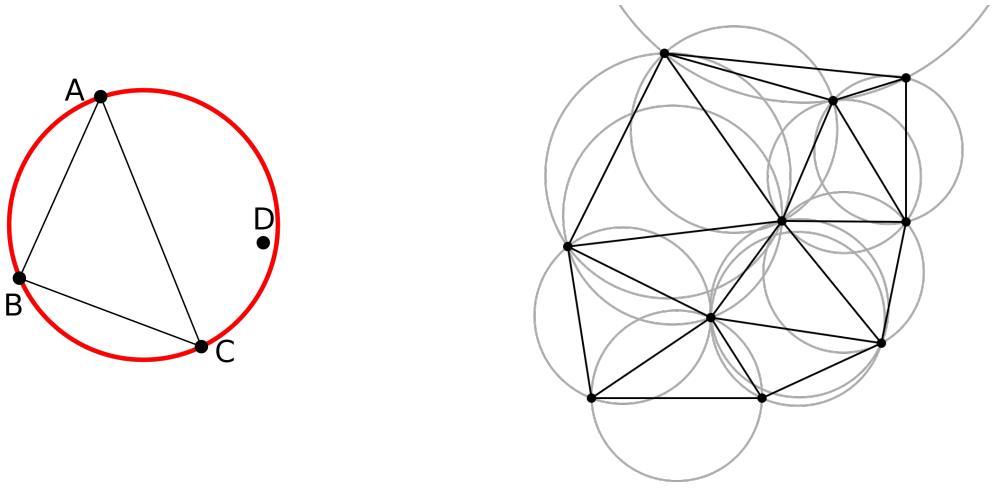

(a) In-circle test for a given triangle [11] (b) Plane with circumcircles shown [12]

Figure 5: Delaunay triangulation

Triangulation is a technique in geometry where a space is divided into smaller triangles. Delaunay triangulation is a method for constructing a triangulation of a set of points in a plane such that no point is inside the circumcircle of any triangle in the triangulation. The idea is to divide the space into triangles, a cubic polynomial is fit to each triangle, and the value of the interpolated point is calculated by evaluating the polynomial at that point

[13, 14]. To detect if any point D lies in the circumcircle of A, B, C in Two-dimensional (2D) space, Delaunay triangulation uses the determinant [15]

$$\begin{vmatrix} x_a & y_a & x_a^2 + y_a^2 & 1 \\ x_b & y_b & x_b^2 + y_b^2 & 1 \\ x_c & y_c & x_c^2 + y_y^2 & 1 \\ x_d & y_d & x_d^2 + y_d^2 & 1 \end{vmatrix} > 0 \tag{6}$$

$$\text{where,} \quad x_n, y_n = \text{coordinates of point N}$$

when A, B, C are sorted in a counter-clockwise order, as shown in the Figure 5.

There are several variations of the Clough-Tocher interpolation method, including bivariate Clough-Tocher interpolation and multi-variate Clough-Tocher interpolation. For each triangle in the formulation formed by the Delaunay triangulation, let (x_a, y_a), (x_b, y_b), and (x_c, y_c) be the coordinates of the triangle's vertices and let z_a, z_b, and z_c be the corresponding function values at those points. Then, the Clough-Tocher interpolation fits a cubic polynomial in the form

$$Z(x, y) = a_0 + a_1 x + a_2 y + a_3 x^2 + a_4 xy + a_5 y^2 + a_6 x^3 + a_7 x^2 y + a_8 x y^2 + a_9 y^3 \tag{7}$$

to the data in each triangle, where the coefficients $a_0, a_1, ..., a_9$ are determined by the data points in the triangle, and the continuity conditions to nearby triangles.

2.3.2 Linear n-dimensional interpolation

Linear n-dimensional interpolation, similar to Clough-Tocher interpolation, is constructed by triangulating the input data points using Delaunay triangulation, however, it is followed by a linear interpolation in N dimensions. For an input set of data points (x, y, z) with function values (u, v), linear n-dimensional interpolation produces a function that can be used to estimate the values of (u, v) at any point within the data range.

An interpolation function relating 2D input to a 3D output

$$f(u, v) = (x, y, z) \tag{8}$$

is created where the known values of $(u_1, v_1), (u_2, v_2)...(u_n, v_n)$ at points (x_1, y_1, z_1), (x_2, y_2, z_2) ... (x_n, y_n, z_n) respectively are used to fit the given function. This function accurately predicts the values of (x_i, y_i, z_i) for any value (u_i, v_i) in the range $(u_1, v_1)(u_n, v_n)$ using

$$f_x(u_i, v_i) = f_x(u_j, v_j) + (u_i - u_j)(v_i - v_j)\left[\frac{f_x(u_k, v_k) - f_x(u_j, v_j)}{(u_k - u_j)(v_k - v_j)}\right] \tag{9}$$

$$f_y(u_i, v_i) = f_y(u_j, v_j) + (u_i - u_j)(v_i - v_j)\left[\frac{f_y(u_k, v_k) - f_y(u_j, v_j)}{(u_k - u_j)(v_k - v_j)}\right] \tag{10}$$

$$f_z(u_i, v_i) = f_z(u_j, v_j) + (u_i - u_j)(v_i - v_j)\left[\frac{f_z(u_k, v_k) - f_z(u_j, v_j)}{(u_k - u_j)(v_k - v_j)}\right] \tag{11}$$

$$f(u_i, v_i) = [f_x(u_i, v_i), f_y(u_i, v_i), f_z(u_i, v_i)] = [x_i, y_i, z_i] \tag{12}$$

where, u_j, v_j = known input coordinates of the point preceding $f(u_i, v_i)$
u_k, v_k = known input coordinates of the point succeeding $f(u_i, v_i)$

These equations can be generalized to more than three dimensions by adding additional terms for each additional dimension.

3 Methodology

The methods used in analysis of the helical gear under load are discussed in this section.

3.1 Method

A python code is written to calculate all the functions, loads and positions. Figure 6 shows the methodology adopted for the current work and the work on the FEA workbench. According to the colour scheme, the orange boxes indicate the input data required, the grey boxes show the interpolated functions, and the blue boxes indicate the calculations done in python. Finally, the green boxes show the steps carried out on ANSYS as the FEA workbench.

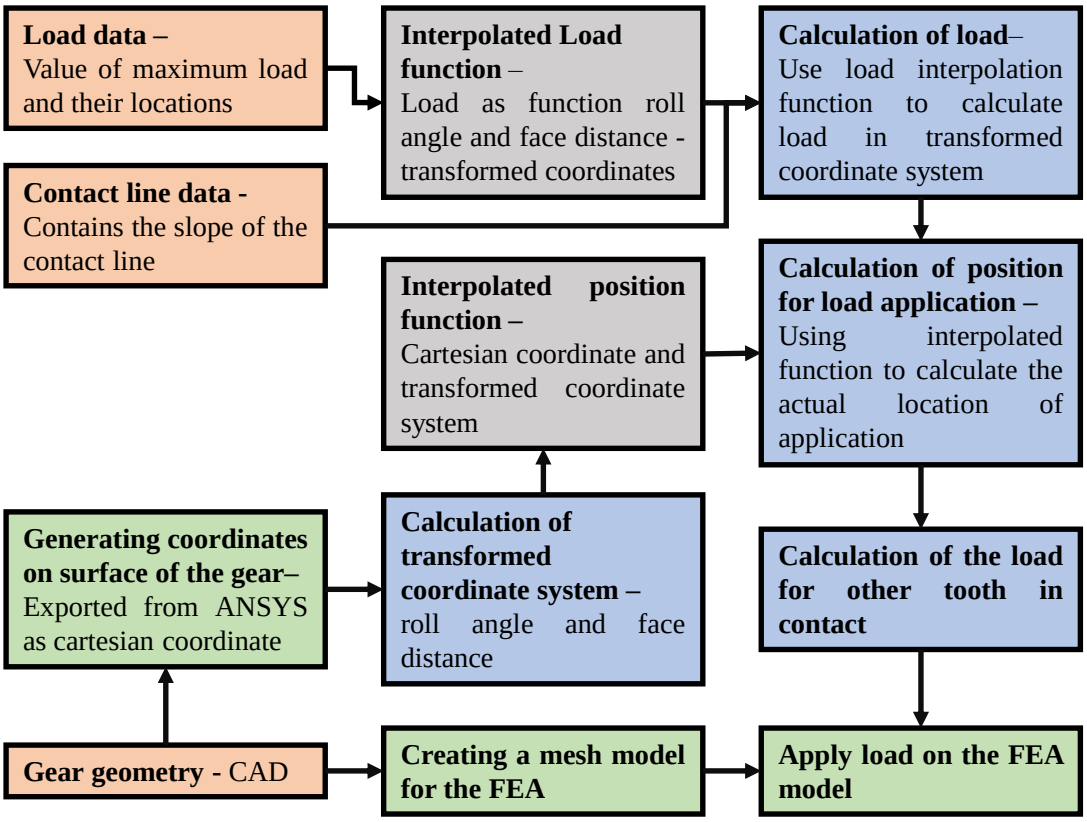

Figure 6: Methodology of the work

3.2 Load data

Figure 7a illustrates the force per unit length along the contact line over the roll angle - face distance plane. These load values are to be integrated along the contact line. This data is read and split into three separate arrays of roll angles ra, face distance fd and load per unit length l.

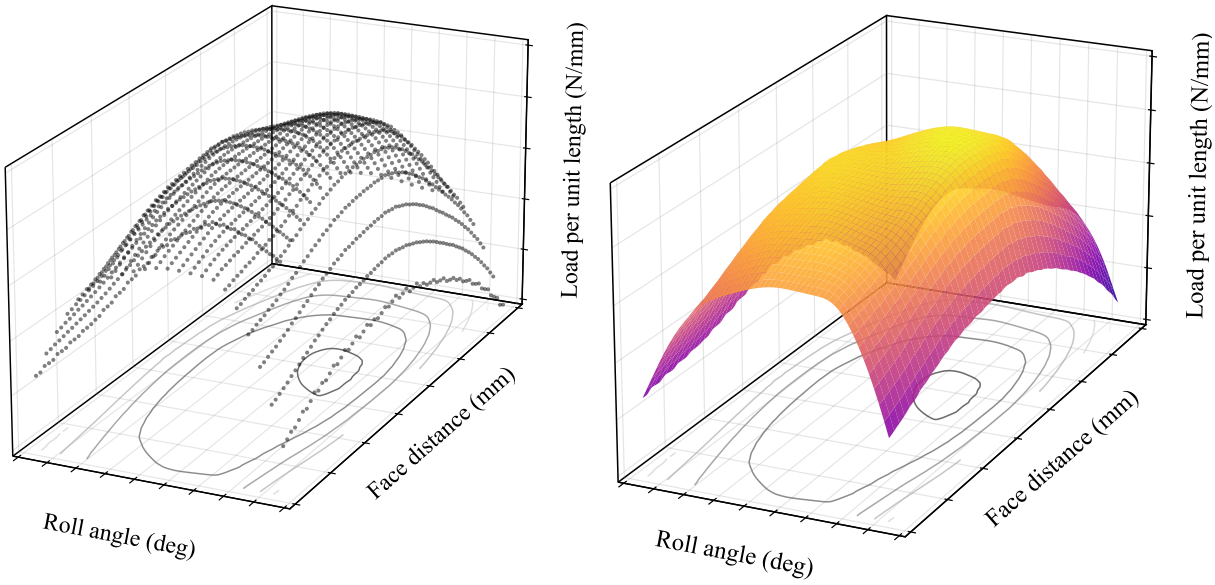

(a) Representation of the load data (b) Representation of an interpolated surface

Figure 7: Load on the gear tooth surface

3.3 Contact line data

As shown in Figure 2, the data for the contact line consists of three lines in the roll angle and face distance plane parallel to all contact lines. The slope of all contact lines for the simulation is the average slope of the three contact lines in the data.

3.4 Interpolated load function

As shown in Figure 7a, the loads form a region with dense point data over the contact region. However, for integration along the contact line, it is necessary to evaluate a function that is a continuous function over the whole range of ra and fd. For this purpose, Clough-Tocher 2D (CT2D) interpolation is used, which is fitted using ra and fd, as well as the corresponding value from the load, yielding function

$$l_x = f_{load}(ra_x, fd_x) \tag{13}$$

where, ra_x, fd_x = input coordinates of point x (i.e., roll angle and face distance)
l_x = estimated value of the force per unit length at that point x

Figure 7b is a surface representation of the function generated. It is assumed that no contact occurs outside the specified range of ra and fd, thus, making the load for all values outside this range zero. The Root Mean Square (RMS) difference between prediction from the function f_{load} and data was 3.26×10^{-15}, which is extremely low.

3.5 Generating coordinates on the surface of the gear

In ANSYS, importing nodal forces onto a geometry is only possible if the point of load application is provided in the coordinate of the geometry. Figure 8 shows the surface on which the load is applied. The gear on the left is the driving gear which rotates in an anti-clockwise direction when viewed from the positive x-axis. The gear in the middle is the investigated gear which rotates in a clockwise direction. Finally, the gear depicted on the right is the driven gear of the system. Figure 8 shows the two main contact surfaces on the investigated gear, which lie on either side. Once the main contact surfaces have been determined, one can export the coordinates of the mesh points on contact surfaces.

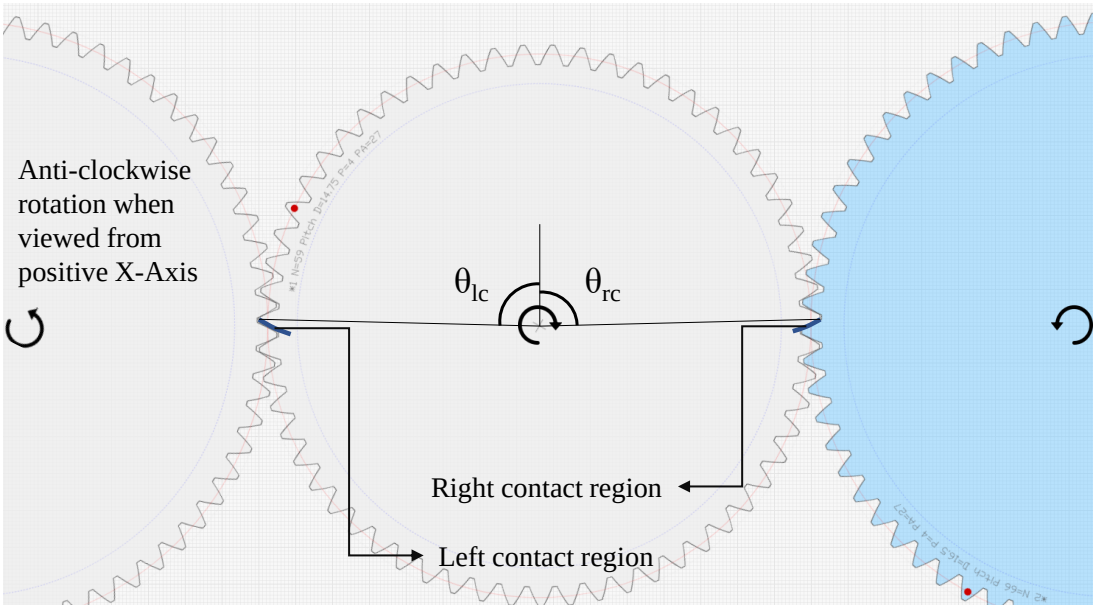

Figure 8: Position of contact regions in the gear assembly

The contact surfaces are exported into a new instance of ANSYS, and a dense mesh of element size ∼0.1 mm is created for the surfaces. It must be ensured that the entire region of $[ra_0, ra_m]$ and $[fd_0, fd_m]$ is covered where ra_0, ra_m are the minimum and maximum values of ra, and fd_0, fd_m are the minimum and maximum values of fd. Using the 'named selection' feature in ANSYS, the coordinates of a mesh that covers the entire contact surface is exported. Special care is taken to ensure that nodes are present on all the edges, otherwise the fit of the interpolation function will exclude the regions that are not enclosed by nodes.

3.6 Calculation of transformed coordinate system

All the coordinates of the points need to be converted into a transformed coordinate system so that the roll angles and face distances of all points can be found. For this purpose, (4) and (5) can be used to calculate the required values of roll angle and face distance.

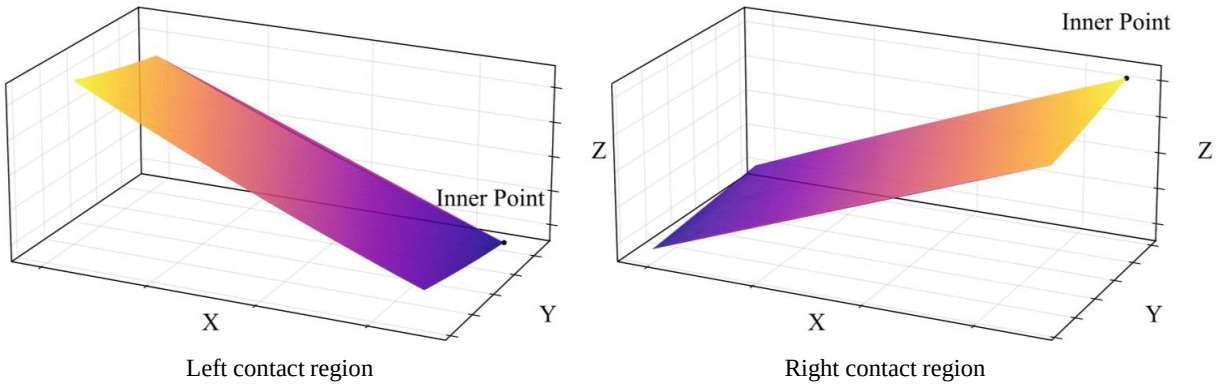

Figure 9: Contact area of the gear tooth with the inner points marked

The point of the gear tooth surface where the face distance is zero is called the inner point. Figure 9 shows the inner points for the two contact regions. For the current calculation, the origin must be at a point where the axis of the gear meets the plane at which the face distance is zero. The x-component of the inner point is subtracted from the x-component of all the points on the contact surface. It effectively moves the origin to the plane of the 'inner point'. Further, the face distance and roll angles for all the points are calculated.

3.7 Interpolated position function

Calculation of the points of load application on the surface of the gear tooth is done using the values of roll angle and face distance with equations (2), (3) and (5). However, many gear designs, including the one used in this study, have micro-geometries on their tooth surface. This reason prevents the calculation of points on the gear tooth surface accurately. Therefore, to find the position of the load application accurately, a linear n-dimensional interpolation function, f_{pos}, is defined such that

$$(x_x, y_x, z_x) = f_{pos}(ra_x, fd_x) \tag{14}$$

where, ra_x, fd_x = input coordinates of a point x (i.e., roll angle and face distance)
x_x, y_x, z_x = estimated value of the cartesian coordinates of point x

The values of the mesh node coordinates (x_x, y_x, z_x) and their corresponding (ra_x, fd_x) calculated in the previous section are used to fit the n-dimensional interpolation function. This calculation is a bijective transformation from a cartesian coordinate system to transformed coordinate system consisting of roll angle and face distance. A similar interpolation function, g_{pos}, is created for estimating the coordinates of the right contact area. The mesh coordinates from the actual mesh are then fed into this function to check the prediction accuracy of the two functions. RMS difference between prediction and data is 0.001499 mm and 0.000754 mm for f_{pos} and g_{pos} respectively, which are well under the allowable error limit in ANSYS. In other words, the loads can be imported on to an ANSYS simulation.

3.8 Calculation of load

For the work undertaken, line load needs to be integrated along the line of contact to find the forces at different points on the roll angle and face distance plane. The direction and the initial position of the contact line for their corresponding transformed coordinate origin have been shown in Figure 10. The origin of the transformed coordinate system is the point at which the roll angle and face distance are minimum at (ra_0, fd_m). The contact line for the left contact region starts at (fd_0, ra_m) with a positive slope and the contact line for the right contact region starts at (fd_m, ra_m) with a negative slope.

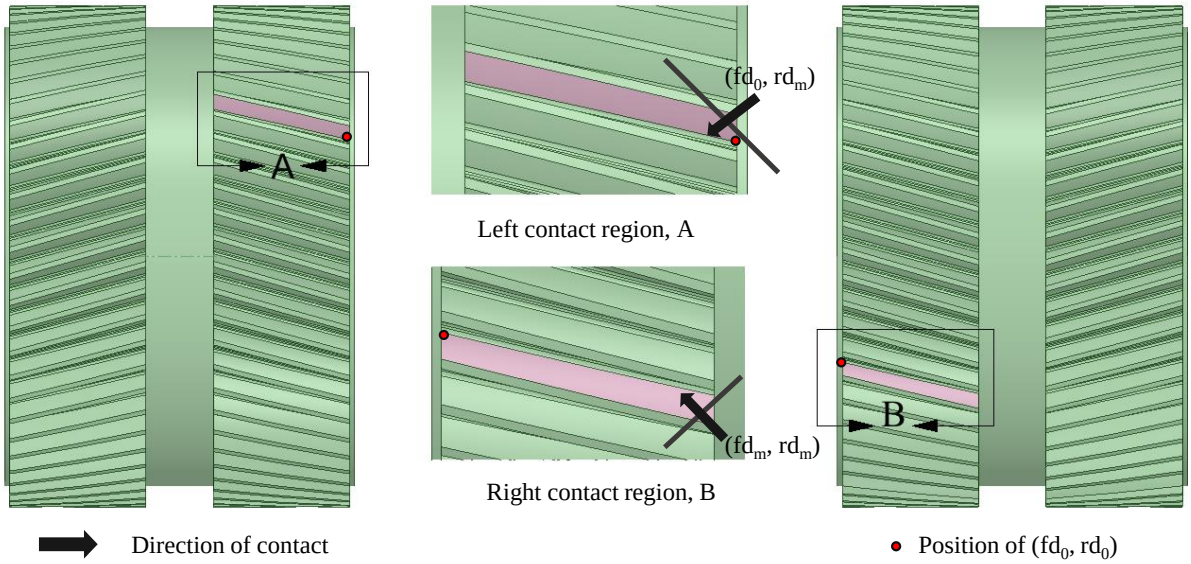

Figure 10: Contact area of the gear tooth with the transformed origin points

3.8.1 Relation between roll angle and roll distance

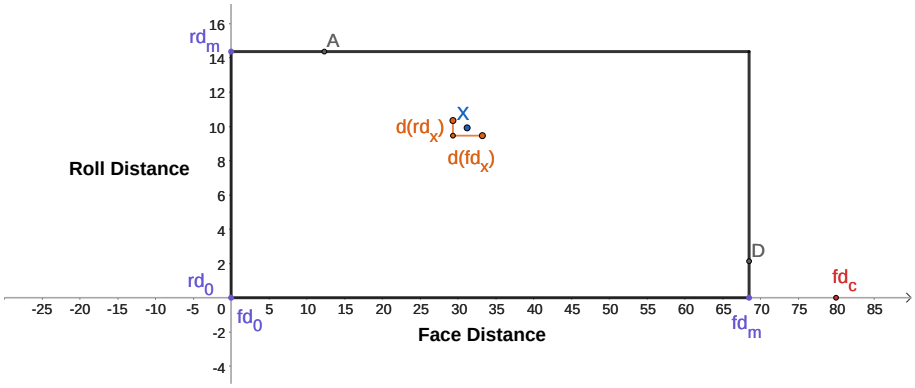

Figure 11: Roll angle vs face distance plot for the right contact region

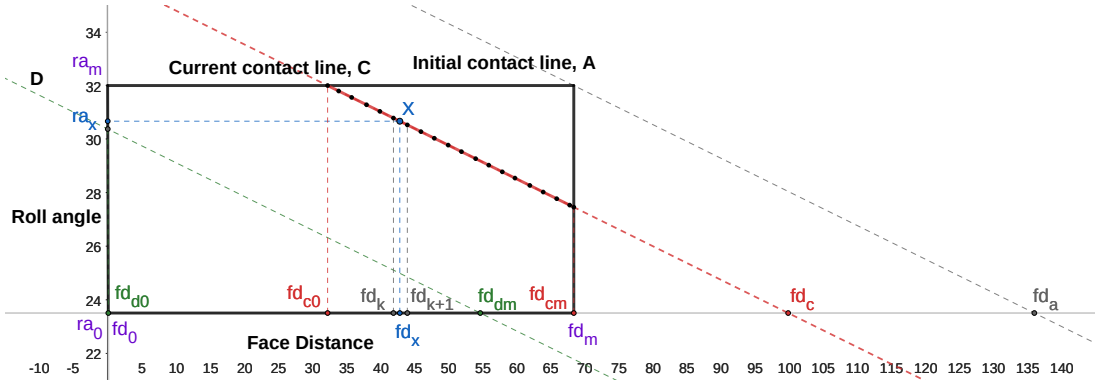

Figure 12: Roll angle vs face distance plot for the right contact region

For converting the load from force per unit length to force, f_{load} is integrated along the contact line. However, the roll angle must be converted to a parameter called roll distance for calculating any distance on the gear face. Roll distance rd is the distance between the base of the involute to the point on the gear tooth along the involute curve. Therefore, roll distance at point x is

$$rd_x = \frac{R_b}{2}\left(\frac{\pi}{180}\right)^2 (ra_x^2 - ra_0^2) \tag{15}$$

where, R_b = Base circle radius in mm
ra_x = roll angle of a point x in degrees
ra_0 = Minimum value of roll angle in degrees
rd_x = roll distance of a point with ra_0

in which roll distance rd_0 is set as zero at ra_0. From Figure 12, roll angle at any point x is

$$ra_x = m \cdot (fd_x - fd_c) + ra_0 \tag{16}$$

where, fd_x = face distance of a point x in mm
m = slope of the contact line
fd_c = intercept of contact line with ra_0 line.

From (15) and (16) a relationship

$$rd_x = \left(\frac{\pi}{180}\right)^2 \frac{R_b}{2}\left[[m \cdot (fd_x - fd_c) + ra_0]^2 - ra_0^2\right] \tag{17}$$

is found between fd_x and rd_x. Using the (17), the slope of the roll distance vs face distance line at a point X along the contact line, m_{rdx}

$$m_{rdx}(fd_x) = \frac{\mathrm{d}(rd_x)}{\mathrm{d}(fd_x)} = \left(\frac{\pi}{180}\right)^2 R_b.m[m.(fd_x - fd_c) + ra_0] \tag{18}$$

is calculated.

3.8.2 Integration of load

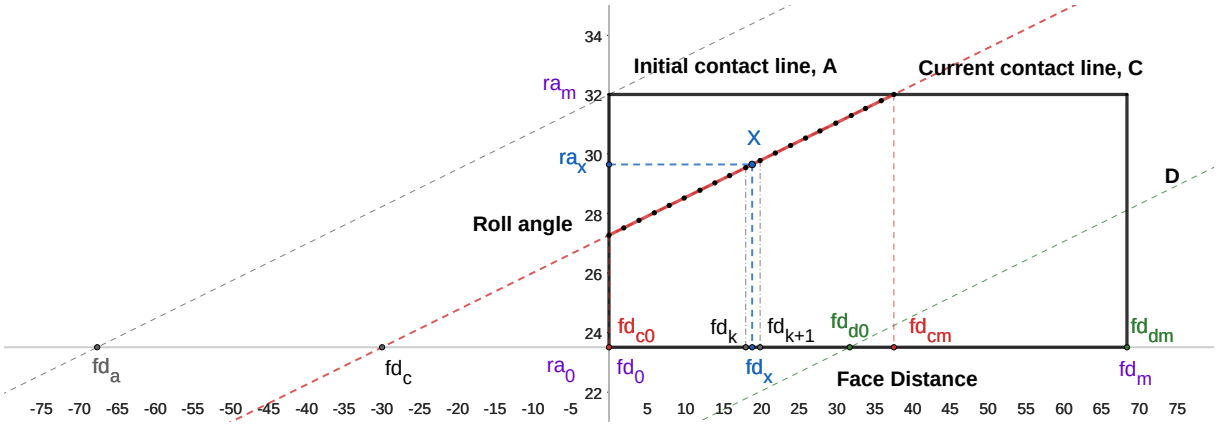

Figure 13: Roll angle vs face distance plot for the left contact region

As mentioned earlier, the forces at different points need to be calculated by integrating force per unit length along the contact line. Figure 13 shows the region roll angle vs face distance plot with the rectangle demonstrating the region in where the force per unit length values are known. Therefore, to calculate the nodal forces along the line of contact, the current contact line, C, in the region is plotted. The contact line can be identified using the intercept fd_c with the line corresponding to ra_0. The contact line is then split into smaller line segments, as shown in the Figure 13. Force at each segment is calculated by integrating f_{load} as

$$F_x = \int_{fd_k}^{fd_{k+1}} f_{load}(ra_x, fd_x) \cdot \frac{d(rd_x)}{d(fd_x)} \cdot d(fd_x) \tag{19}$$

Using (17),

$$F_k = \int_{fd_k}^{fd_{k+1}} f_{load}(ra_x, fd_x) \cdot m_{rdx}\ fd_x \cdot d(fd_x) \tag{20}$$

where, F_k = force on the k segment
fd_k = starting fd of the segment
fd_{k+1} = starting fd of the segment

3.8.3 Components of the load

In a helical gear, the forces on the gear teeth act in a direction normal to the gear surface. The forces on the gear teeth have three main components: tangential forces F_t, radial forces F_r and axial forces F_a. These forces align with the x, y, and z axes if the tooth is at the top of the gear as shown in Figure 14.

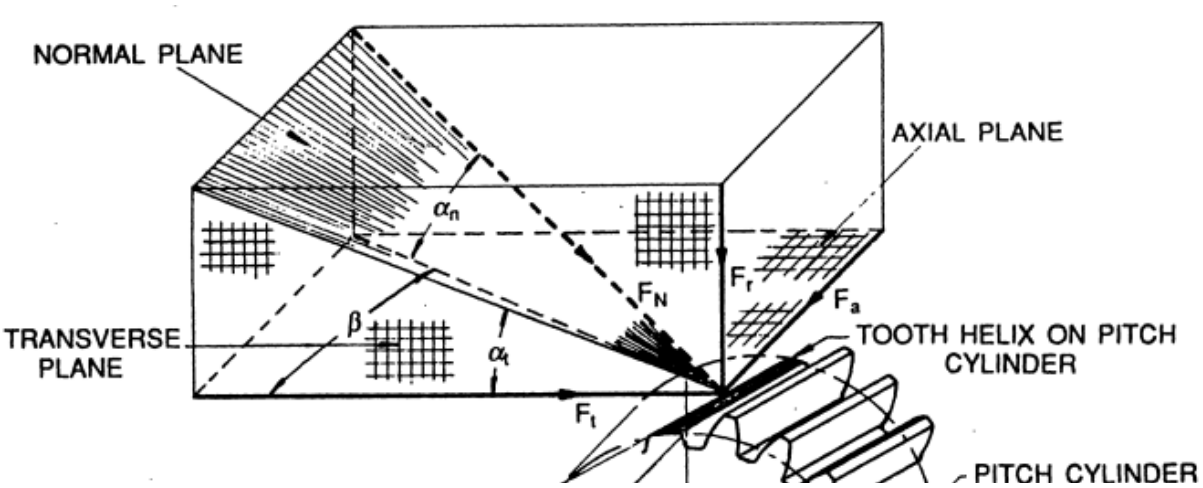

Figure 14: Gear tooth forces on helical gears [16]

The components of a force F

$$F_a = F\ cos(\alpha) \cdot sin(\beta) \tag{21}$$

$$F_t = F\ cos(\alpha) \cdot cos(\beta) \tag{22}$$

$$F_r = -F\ sin(\alpha) \tag{23}$$

for a gear tooth at the top as shown in Figure 14.

However, as shown in Figure 8, contact teeth are at angles of θ_{lm} and θ_{rm} for left and right contact regions respectively. The component of the force for a segment k is evaluated by rotating the force vector

$$\overrightarrow{F_k} = \begin{bmatrix} F_{kx} \\ F_{ky} \\ F_{kz} \end{bmatrix} = \overrightarrow{F} \cdot \mathbf{R_x}(\Theta) = \begin{bmatrix} F_a \\ F_t \\ F_r \end{bmatrix} \cdot \begin{bmatrix} 1 & 0 & 0 \\ 0 & cos\ \Theta & -sin\ \Theta \\ 0 & sin\ \Theta & cos\ \Theta \end{bmatrix} \tag{24}$$

where, $\Theta = \theta_{lm} + \theta_k$
DEF = Assumed integer (200 in this study)
$\mathbf{R_x}$ = Rotation matrix around the X axis

by Θ, which is the sum of contact teeth angle θ_{lm} and the angle between normals at point k and the pitch circle θ_k.

For the right contact region, the value of tangential, radial and axial forces will be in the opposite direction of the ones for the left contact region, because the loading surface is on the opposite face of the gear tooth.

3.8.4 Locating the point of load application

Using the interpolation function f_{pos}, the point of load application in the coordinates of the gear geometry can be found. For the k^{th} segment, the force is applied at a position on the contact line at which the face distance of $fd_k + \frac{\Delta}{2}$. Here Δ is the change in fd for the segment.

$$(x_k, y_k, z_k) = f_{pos}\left(ra'_k, fd'_k\right) \tag{25}$$

$$\begin{aligned} \text{where,} \quad ra'_k &= \text{value of roll angle at } \left(fd_k + \tfrac{\Delta}{2}\right) \\ fd'_k &= fd_k + \tfrac{\Delta}{2} \end{aligned}$$

Here (ra'_k, fd'_k) is the coordinate of application of force in the transformed coordinates and (x_k, y_k, z_k) is the coordinate of application of force in the cartesian coordinates corresponding to the gear geometry.

3.8.5 Calculating load for all the segments in the region

The calculations mentioned in Subsection 3.8.1 to 3.8.4 are repeated for all the segments of the contact line and all the lines in the contact region. Distance between each line can be varied by changing the values of fd_c. In this work, the change in the fd_c value is kept the same as the change in fd for the segment Δ. An assumption has to be taken here regarding the value of Δ. The duration of a given load increases with the increase in Δ. For this study, the value is

$$\Delta = \frac{\left(\frac{fd_m - fd_0}{2} + \left|fd_a - \frac{fd_m - fd_0}{2}\right|\right)}{DEF} \tag{26}$$

$$\begin{aligned} \text{where,} \quad fd_a &= \text{farthest intercept of contact line that also falls in the contact region} \\ DEF &= \text{number of times the range is split (200 in this study)} \end{aligned}$$

Further, the time t taken by the contact line to move from fd_a to fd_c is

$$t = \frac{ra_x - ra_0}{60.RPM} \tag{27}$$

$$\text{where,} \quad RPM = \text{Rotations per minute}$$

and it is assumed that when fd_a is equal to fd_c, time is set to zero. Finally, a 2D matrix comprising of the component of force, position of application of force, roll angle ra'_k, face distance fd'_k, time and current face distance fd_c is created.

3.9 Calculating the load for other teeth in contact

Once a 2D list of all the loads acting on the gear are calculated, they can easily be exported to other teeth by rotating each force vector, $\overrightarrow{F_k}$, and position vector, $\overrightarrow{k}$, with the angle

between two neighbouring teeth Θ_{teeth}. This angle can be calculated using the number of gear teeth Z_t. The fd_c value for the gear teeth also changes with the value of Θ_{teeth}.

$$\Theta_{teeth} = \frac{360}{Z_t} \tag{28}$$

$$\overrightarrow{F'_k} = \overrightarrow{F_k}.\mathbf{R_x}(\Theta_{teeth}) \tag{29}$$

$$\overrightarrow{k'} = \overrightarrow{k}.\mathbf{R_x}(\Theta_{teeth}) \tag{30}$$

$$fd'_c = fd_c - \frac{\pi.\Theta_{teeth}}{180\ m} + fd_0 \tag{31}$$

$$t' = t - \frac{\Theta_{teeth}}{60\ RPM} \tag{32}$$

where, Θ_{teeth} = Angle between two neighbouring teeth
F'_k = force on teeth Θ_{teeth} away
k' = coordinates of point k on Θ_{teeth} away
fd'_c = fd_c value for on gear teeth Θ_{teeth} away
t' = time corresponding to k'

All these loads are mirrored on the mid-plane of the gear geometry to evaluate the loads on the other helix. In the current case, only the x-components on load and positions need to be changed between k and k' where k is a point on the main helix and k' is a point on the opposite helix.

$$x'_k = x_k - W_g + 2W_t \tag{33}$$

$$\overrightarrow{F'_{xk}} = -\overrightarrow{F_{xk}} \tag{34}$$

where, W_g = Width of the gear from end to end including both helix
W_t = Width of the single helical teeth
x_k = x- coordinate of point k
x'_k = x- coordinate of point k'
F_{xk} = x- component of force on point k
F'_{xk} = x- component of force on point k'

The coordinates and the forces on all the teeth in contact were calculated and imported into ANSYS using the 'external data' component system.

4 Results

In this section, the results of the work are analysed.

4.1 Analysing the position of load application

The calculations made in section 3 were verified using python by plotting the coordinates of the nodes of the mesh and then positioning the calculated locations of the load on top of them. Figure 15 shows the plotting for the left and right contact regions and clearly illustrates that all the points lie on the surface of the plotted gear mesh.

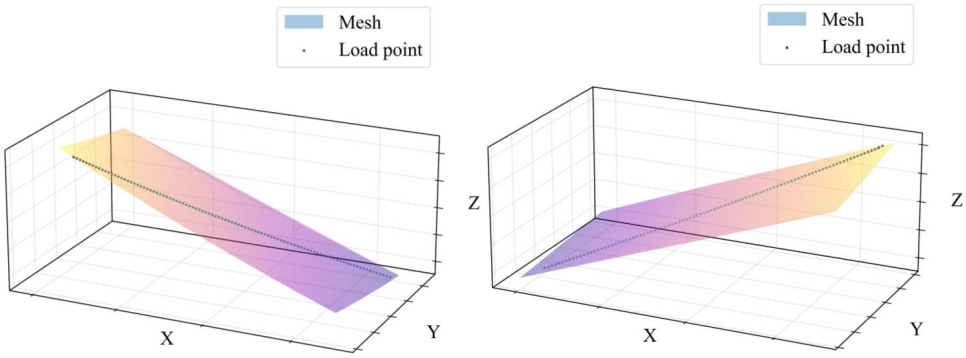

Figure 15: Position of loads on the left contact region (Left) and right contact region (Right) visualized with Python

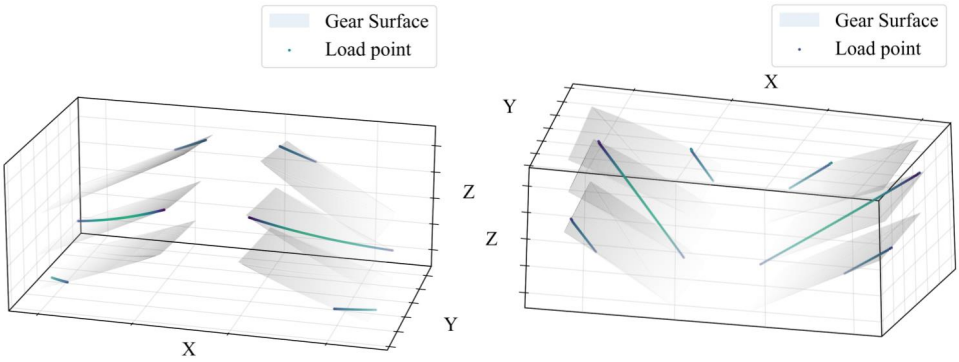

Figure 16: Checking the position of loads on the gear at all contact regions with Python

The locations were also verified for all the 12 contact regions active at any given time using the same process of plotting their respective mesh node coordinates and following it up with plotting the coordinates of calculated positions of load application, as shown in Figure 16. Finally, the forces are imported onto the surface of the gear tooth. They aligned perfectly with the geometry, as shown in Figure 17 and 18. If the loads did not align with the geometry, they would have failed to load.

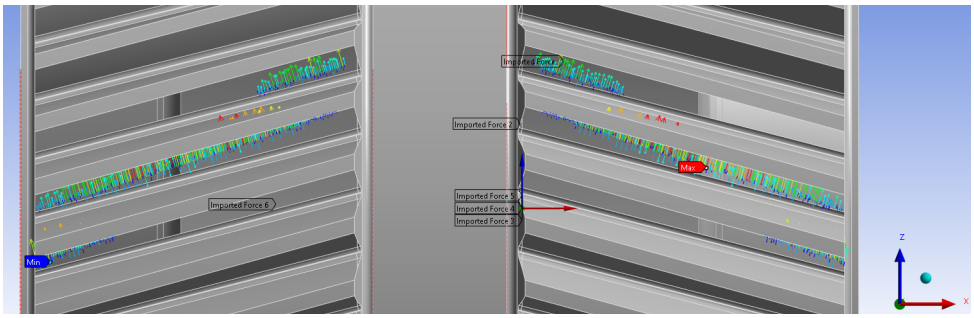

Figure 17: Position of loads on the gear - ANSYS

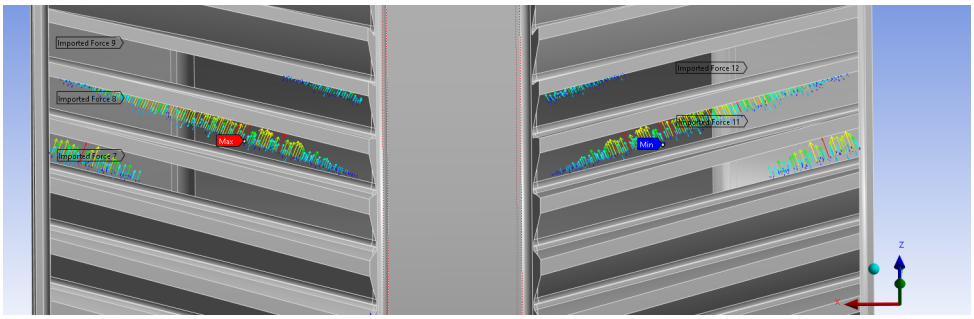

Figure 18: Checking the position of loads on the gear - ANSYS

5 Conclusion

The main task undertaken in this work has been to calculate the quasi-static load on a double helical gear under uniform speed. The load and contact line data in the transformed coordinate system comprising of roll angles and face distances are provided for a double helical gear. The loads provided are force per unit length values given in a range of roll angle and face distance mesh grid. To convert the discrete point data to a continuous function, a CT2D Interpolation function is used. The loads per unit length are converted to nodal forces by integrating the interpolated function along a line of contact for each segment. The position of load application is determined by a multi-dimensional linear interpolation function that is fitted using the data from a dense mesh and their calculated roll angles and face distances. The point of application of force is set as the mid-point of the segment. Further, tangential, axial, and radial forces are calculated for the gear tooth and rotated to match the position of the gear. The loads are computed for all the active gear teeth by rotating or mirroring the loads and position vectors. Finally, the calculated loads are verified using python by plotting the coordinates of the mesh surfaces of the gear tooth and plotting the load positions on top of them. The loads are imported into ANSYS and it is verified that the load is acting on the surface of the gear.

5.1 Future work

The calculations undertaken in this study will be used for replicating the dynamic loads acting on the gear. These calculations make a static simulation of a single gear possible,

which will reduce the computational time for the simulation considerably compared to a three-gear dynamic simulation. Further, the simulations will be used to determine the position and propagation direction of cracks on the gears. Loads on the cracked gear will be calculated using analytical time-varying mesh stiffness methods. Finally, Phase field modelling will be used to understand the direction of propagation of cracks and will be compared to stress intensity factor method.

References

[1] AL Mohd Tobi and AE Ismail. 'Development in Geared Turbofan Aeroengine'. In: *IOP Conference Series: Materials Science and Engineering*. Vol. 131. 1. IOP Publishing. 2016, p. 012019.

[2] American Gear Manufacturers Association et al. 'AGMA standard 2001-D04'. In: *Fundamental rating factors and calculation methods for involute spur and helical gear teeth* (2004).

[3] American Gear Manufacturers Association et al. 'AGMA 908-B89: Geometry Factors for Determining the Pitting Resistance and Bending Strength of Spur, Helical and Herringbone Gear Teeth'. In: *Alexandria, USA: American Gear Manufactures Association* (1989).

[4] ISO Standard. '6336-1: 2006'. In: *Calculation of load capacity of spur and helical gears, Part 1: Basic principles, introduction and general influence factors* (2006).

[5] ISO Standard. '6336-2: 2006'. In: *Calculation of load capacity of spur and helical gears, Part 2: calculation of surface durability (pitting)* (2006).

[6] ISO Standard. '6336-3: 2006'. In: *Calculation of load capacity of spur and helical gears, Part 3: Calculation of tooth bending strength* (2006).

[7] Amit D Modi and KR Gawande. 'Optimization and SN life cycle analysis of helical gear with nickel alloy MP35N'. In: *IOP Conference Series: Materials Science and Engineering*. Vol. 1258. 1. IOP Publishing. 2022, p. 012022.

[8] Jiaxing Zhan, Mohammad Fard and Reza Jazar. 'A quasi-static FEM for estimating gear load capacity'. In: *Measurement* 75 (2015), pp. 40–49.

[9] MR Lias et al. 'Quasi-static modeling of spur gear time varying strength analysis'. In: *ARPN Journal of Engineering and Applied Sciences* 12 (2016), pp. 1938–47.

[10] *Calculation of involute gears*. https://www.tec-science.com/mechanical-power-transmission/involute-gear/calculation-of-involute-gears/. "[Online; accessed 21-Dec-2022]". 2018.

[11] Wikimedia Commons. *File:Point inside circle - Delaunay condition broken - Labelled.svg — Wikimedia Commons, the free media repository*. [Online; accessed 21-January-2023]. 2020. URL: https://commons.wikimedia.org/w/index.php?title=File:Point_inside_circle_-_Delaunay_condition_broken_-_Labelled.svg&oldid=442848012.

[12] Wikimedia Commons. *File:Delaunay circumcircles vectorial.svg — Wikimedia Commons, the free media repository*. [Online; accessed 21-January-2023]. 2022. URL: \url{https://commons.wikimedia.org/w/index.php?title=File:Delaunay_circumcircles_vectorial.svg&oldid=651563338}.

[13] Shaoming Wang. 'A smooth surface interpolation to 3D triangulations'. In: *Journal of computational and applied mathematics* 163.1 (2004), pp. 287–293.

[14] Praveen Kashyap. 'Improving clough-tocher interpolants'. In: *Computer aided geometric design* 13.7 (1996), pp. 629–651.

[15] Leonidas Guibas and Jorge Stolfi. 'Primitives for the manipulation of general subdivisions and the computation of Voronoi'. In: *ACM transactions on graphics (TOG)* 4.2 (1985), pp. 74–123.

[16] Gitin M Maitra. *Handbook of gear design*. Tata McGraw-Hill Education, 1994.